

ENHANCED BOILING HEAT TRANSFER INSIDE HORIZONTAL AND VERTICAL TUBES

Rafaela Frota Reinaldo(*) – rafaela@labsolar.ufsc.br

Vinícius Fernando Kuser(*) – kuser@iname.com

Hein Auracher – auracher@iet.tu-berlin.de

Technical University of Berlin, Germany

Júlio César Passos(*) – jpassos@emc.ufsc.br

(*)Universidade Federal de Santa Catarina, Departamento de Engenharia Mecânica

LABSOLAR-NCTS

88010-970 – Florianópolis, SC, Brazil

***Abstract.** This work presents experimental results for R113 nucleate pool boiling inside smooth and grooved vertical and horizontal aluminum tubes, at atmospheric pressure and moderate heat flux ($<45 \text{ kW/m}^2$). Heat flux and wall temperature related to the nucleation phenomenon are obtained. For the nucleate boiling regime, the effects of R113 subcooling, surface effect and tube orientation are investigated. Smooth tube experimental heat transfer coefficients are compared with Stephan and Abdelsalam, Cooper, Rohsenow and Forster and Zuber correlations and with grooved tube experimental values. For all tests, heat transfer coefficient is higher in the grooved tube than in the smooth tube. For horizontal orientation, there is an azimuthal temperature gradient due to the existence of different boiling mechanisms on the inside wall of the tube.*

***Keywords :** Boiling, Enhanced surface, Nucleate boiling , Nucleation*

1. INTRODUCTION

Several works (Marto & Lepere, 1982, Thome, 1990, Reinaldo, 1999, Passos & Reinaldo, 2000) consider the nucleate boiling regime for enhanced surfaces and compare the results for similar test conditions with smooth surfaces. Commercial tubes, with different types of surface enhancement, are already used in some refrigeration and air conditioning systems.

The objective of this study is the experimental research of R113 pool boiling heat transfer within smooth and grooved open ended tubes, in vertical and horizontal orientations. The purpose of this study is to analyze a particular grooved enhanced surface by comparison with experimental results obtained, at the same test conditions, for a smooth tube, and with results computed by some empirical correlations.

1.1 Literature review

Enhanced surfaces. Bergles and Webb, see Thome (1990), list eleven techniques to obtain enhanced surfaces, which may be divided into passive and active. Among the passive techniques we may find treated surfaces, rough surfaces by means of an abrasive treatment, extended surfaces and surface tension devices. The heat transfer obtained by an extended surface, such as a finned tube, can be enhanced simply by increasing the wetted surface area. Thus, in this case the boiling heat transfer mechanism under the same test conditions is very similar to the one observed in a plain tube with the same area, see Thome (1990), Hewitt (1998). In order to improve the boiling heat transfer coefficient, special extended surface geometries have been made with, for example, micro fins and special re-entrant cavities, which promote the confinement of the liquid.

The fact that a cavity in a heater wall flooded by a superheated liquid may become a privileged nucleation site if the cavity traps vapor is a quite well known phenomenon (Carey, 1992). The condition to have vapor entrapped by a cavity is to make it difficult for the cavity to be filled by the liquid phase. This depends on surface tension, contact angle, wall material and cavity geometry.

Thome (1990), Stephan (1992) and Carey (1992) present results showing the increase of boiling heat transfer on different enhanced surface geometries, represented by a much lower wall superheating during the nucleate regime, when compared to a smooth surface under the same test conditions.

Correlations. In this section we present four correlations for the nucleate pool boiling regime. These were selected because they are often used and recommended by several authors, (Hewitt (1998), Carey (1992)).

Stephan & Abdelsalam (1998), used dimensional analyses of transport properties of four different groups of fluids. For refrigerant fluids, including R113, the following correlation was obtained:

$$h_{SA} = 207 \frac{k_l}{d_b} \left(\frac{q d_b}{k_l T_{sat}} \right)^{0.745} \left(\frac{\rho_v}{\rho_l} \right)^{0.581} Pr_l^{0.533} R_p^{0.133} \quad (1)$$

where k_l , q , T_{sat} , ρ_l and ρ_v represent the conductivity, heat flux, saturation temperature, liquid density and vapor density, respectively. The term d_b represents the bubble departure diameter and is computed by the following equation:

$$d_b = 0,0149 \theta \left[\frac{2\sigma}{g(\rho_l - \rho_v)} \right]^{1/2} \quad (2)$$

where θ is the vapor/liquid contact angle, which for refrigerants has a recommended value of 35° , and σ and g represent surface tension and gravity acceleration. Equation (1) results of the comparison with nearly 400 experimental data for boiling on horizontal surfaces (flat plate, tubes, cylinder and wire) in the range of fully established nucleate boiling under the influence of the gravity field. The deviation from the experimental values of h and those computed by Eq. (1) is equal to 10.57%.

A very simple correlation from experimental data for saturation nucleate pool boiling was obtained by Cooper (1984), using only reduced pressure, p_r , molecular weight, M , and surface roughness, R_p , see Eq. (3):

$$h_{\text{Cooper}} = 55 p_r^b (-\log p_r)^{-0.55} M^{-0.5} q^{0.67} \quad (3)$$

where $b = 0.12 - 0.4343 \ln R_p$ represents the effect of surface roughness, with R_p in μm , q refers to heat flux, in W/m^2 and h_{Cooper} is in $\text{W}/(\text{m}^2\text{K})$. For R-113, $p_{\text{critical}} = 3.411 \times 10^6 \text{ Pa}$ and $M = 187.4 \text{ kg}/\text{kmol}$. The deviation of h_{Cooper} values computed by Eq. (3) from the corresponding experimental data is equal to $\pm 20\%$.

The Rohsenow correlation, see Hewitt (1998), considers the Nusselt number in function of the bubble departure diameter, see Eq. (2), as an analogy with the one phase forced convection, equal to a power product law of Reynolds number, in function of the vapor superficial velocity, and the liquid Prandtl number. This correlation is given as:

$$h_R = \mu_l h_{lv} \left[\frac{\sigma}{g(\rho_l - \rho_v)} \right]^{-1/2} \left(\frac{c_{pl}}{C_{sf} h_{lv} Pr^s} \right)^3 \Delta T_w^2 \quad (4)$$

where the C_{sf} coefficient depends on the liquid/solid combination and the exponent s is equal to 1 for water and 1.7 for others fluids. In the present work $C_{sf} = 0.013$ was considered.

Similarly to the Rohsenow correlation, the Nusselt number in the Forster and Zuber (1955) correlation, is a function of the Reynolds and Prandtl numbers. However, characteristic dimension and velocity are determined by the theory of bubble growth. This correlation is given as,

$$h_{FZ} = 0,00122 \left(\frac{k_l^{0.79} c_{pl}^{0.45} \rho_l^{0.49}}{\sigma^{0.5} \mu_l^{0.29} h_{lv}^{0.24} \rho_v^{0.24}} \right) [T_p - T_{\text{sat}}(p_1)]^{0.24} \Delta p_{\text{sat}}^{0.75} \quad (5)$$

where Δp_{sat} is the difference in saturation pressure corresponding to a difference in saturation temperature equal to wall superheat.

The correlations described can be expressed as follows:

$$h = C q^n \quad (6)$$

Table 1 shows the coefficient C and the exponent n for the R113 at atmospheric pressure (for the R113, $k_l = 0.0705 \text{ W}/(\text{m K})$, $c_{pl} = 984 \text{ J}/(\text{kg K})$, $\rho_l = 1507 \text{ kg}/\text{m}^3$, $\rho_v = 7.46 \text{ kg}/\text{m}^3$, $\sigma = 0.017 \text{ N}/\text{m}$, $\mu_l = 516 \times 10^{-6} \text{ Pa s}$, $Pr_l = 7.2$, $h_{lv} = 143.8 \text{ kJ}/\text{kg}$ and $T_{\text{sat}} = 320.75 \text{ K}$).

Table 1. Constants in Equation (6)

Authors	C	n
Stephan & Abdelsalam (1980)	1.16	0.745
Cooper (1984)	2.66	0.670
Rohsenow 1 ($s = 1$)	3.00	0.670
Rohsenow 2 ($s = 1.7$)	0.75	0.670
Forster & Zuber (1955)	9.90	0.520

Table 1 shows that, except for the Forster & Zuber correlation, n is comprised within the range value of 0.6 to 0.8 which, according to Stephan (1992), is the relation between h and q , in the Eq. 6, which characterizes the intensive nucleate boiling regime.

2. EXPERIMENT

2.1 Test section

The R113 boiling tests were carried out inside two open-ended aluminum tubes, with either smooth or grooved internal surfaces, in the vertical and horizontal orientations, immersed in R113 in a Pyrex glass container, as described by Reinaldo (1999). The working fluid (R113) bulk temperature was controlled by a serpentine that circulated water controlled by a LAUDA thermal bath covering the external surface of the Pyrex glass.

The smooth tube had the following dimensions: inside diameter (ID), outside diameter (OD) and length (L) equal to 16.64 ± 0.05 , 18.99 ± 0.04 and 40 mm, respectively. The smooth tube was anodized and the average roughness R_p of the inside surface was $2.2 \mu\text{m}$. The grooved tube had the following dimensions: ID = 15.88 ± 0.04 , OD = 19.11 ± 0.04 and L = 40 mm. The internal surface of the grooved tube had circumferencial grooves made by ERNO of Germany. The main dimensions of the grooves were $33 \pm 7 \mu\text{m}$ of opening and $310 \pm 59 \mu\text{m}$ of depth with a step of $215 \mu\text{m}$.

The aluminum tube was monitored with five type E (Chromel-Constantan) thermocouples (Tc 1 to 5), whose cable diameters equal 0.127 mm, attached with OMEGA cement, inside 0.8 mm diameter holes, with 0.2 mm of depth on the outer wall of the tubes. Thermocouples locations on the test section are shown in Fig. 2. The heating of each aluminum tube was accomplished by two electrical skin heaters, (produced by the Laboratory of Porous Media and Thermophysical Properties (LMPT) of Federal University of Santa Catarina (UFSC)), which were attached on the outer surface of the tube and covered by a PVC tube. The electrical skin heaters are connected in parallel, and their equivalent resistances for smooth and grooved tubes were equal to 5.32Ω and 5.17Ω , respectively. Finally, this set was covered by a second PVC tube and the annular space between the PVC tubes was insulated. A type E thermocouple (Tc₆) was located on the outside surface of the internal PVC tube. A differential type K thermocouple, Tc₇, allowed for the measurement of the equivalent temperature difference between the outside surface of the internal

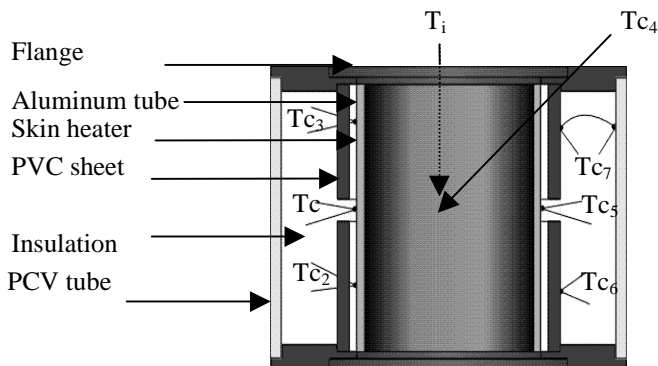


Figure 1. Test section

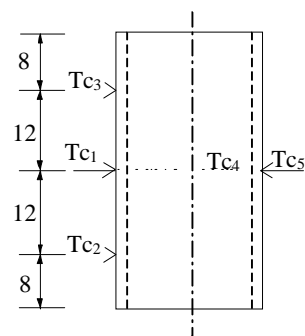


Figure 2. Thermocouple locations

PVC tube and the inner surface of the external PVC tube. Heating losses from the outside of the test section were estimated by Tc₆ and Tc₇ signals.

Two type E thermocouples were placed in the R-113, one of them on the axis of the tube, T_i, (at the middle of the tube length) and the second outside the tube. The thermocouple signals and the voltage at the skin heater ends were recorded by a HP3497A data acquisition system and then transferred to a microcomputer. The electrical input to the test section was delivered by a HP6030A (0-200 V and 0-17A) power supply controlled by a microcomputer.

2.2 Procedure

The test section heating was controlled by a C language program, allowing a voltage step varying from zero up to a fixed value, V₁. The data were acquired after the system had reached a steady state condition. After the first data acquisition, a new level voltage, V₂, was applied and new data was acquired. Some tests were performed with a continuous variation of the voltage as a ramp function.

Experimental uncertainty. The experimental uncertainty of type E thermocouples was equal to ± 0.6 K and were measured and computed, with a 95% confidence level, following the procedure described by Holman (1989) and ASME (1986) and presented by Reinaldo (1999).

The experimental uncertainty of the heat transfer coefficient value was computed following the procedure presented by Kline (1985) and Holman (1989). The relative uncertainty values for q are equal to ±3.5% and ±2% for a heat flux of 5 and 45 kW/m², respectively. The relative uncertainty values for the experimental heat transfer coefficient, h, are equal to ± 11 % and ± 6 %, for a heat flux of 5 and 45 kW/m², respectively.

Data reduction. The mean heat transfer coefficient, h, is computed in function of the difference between the mean wall temperature, T_w, and the saturation temperature, T_{sat}, as follows:

$$h = \frac{q}{(T_w - T_{sat})} \quad (7)$$

where q represents the mean heat flux delivered to the R113, on the internal surface of the tube. For the vertical tube, T_w represents the average of temperatures Tc1 to Tc5, whereas for the horizontal tube, T_w is computed as (T_{bottom} + Tc₄ + Tc₅)/3, where T_{bottom} is the average of Tc₁, Tc₂ and Tc₃ temperatures.

3. RESULTS AND DISCUSSION

3.1 Nucleation

In this section the effects of the surface, surface orientation and subcooling on the transition between the natural convection and the nucleate regime are considered, see (Reinaldo, 1999).

Figure 3a shows the net heat flux delivered to R-113 against time, for a vertical smooth tube, with T_{bulk} equal to 22.0 °C (25.6 °C of subcooling). Figure 3b shows the average wall temperature against time as a result of the heating showed in Fig. 3a. The average wall temperature increases during the first 20 s and begins to stabilize near 60 °C (15.4 °C of superheating). At circa 110 s

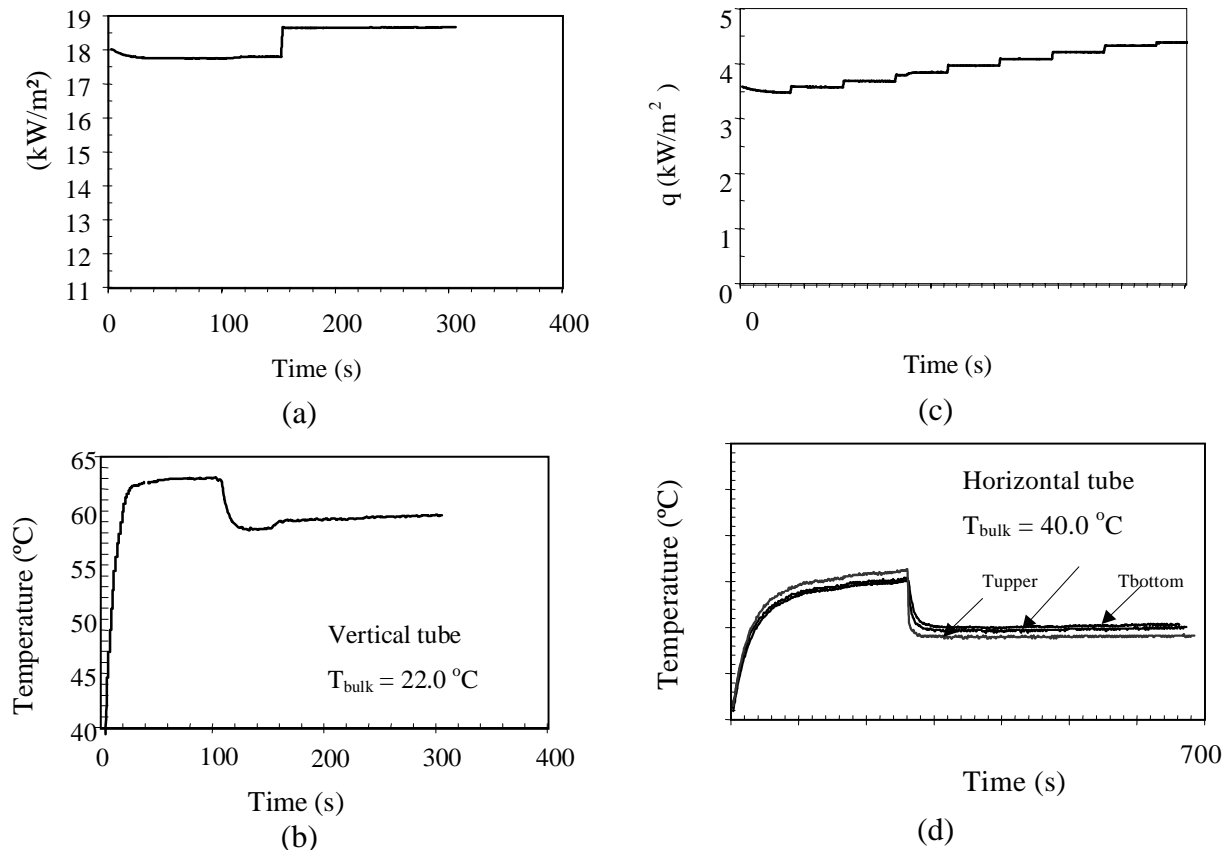


Figure 3 – a,c) Time evolution of the heat flux; b,d) Time evolution of the wall temperatures

the average wall temperature decreases without a change in the heating level, as a consequence of the onset of boiling on the inside surface of the tube. The creation and departure of vapor bubbles promote the agitation of the liquid near the tube wall, allowing the increase in heat transfer which characterizes the nucleate boiling regime. At circa 150 s, the heat flux is increased by 5 % and wall temperature increases in nearly 2 °C.

Figure 3c shows the net heat flux delivered to R113, with T_{bulk} equal to 40.0 °C (7.6 °C of subcooling), for a horizontal smooth tube. The increase in heat flux was obtained, step by step, at every 80th second. The temperatures indicated by three thermocouples located at the top, middle and bottom of the horizontal tube are shown in Fig. 3d. During natural convection, the temperature at the top is higher than those at the other locations, as expected. After the onset of boiling there is a reversal in the temperatures, with a lower temperature being found at the top. This effect is related to the liquid vapor configuration inside the tube, at the top, and the mechanism of vaporization of a film liquid between an elongated bubble and the tube wall (Reinaldo, 1999; Passos & Reinaldo, 2000). At the middle and bottom regions of the wall, the nucleate regime was characterized by isolated bubbles and big bubbles escaping through the ends of the tube.

Main results of nucleation analysis are presented in Table 2. The data line with (*) was obtained, at least, eight months after the first test and after cleaning the test section; the wall superheating for eight tests were comprised between 4.6 and 10.2 K. Data for the vertical grooved tube do not show a clear influence of the liquid subcooling, or of T_{bulk} , on the

superheating needed to start the nucleate boiling. Moreover, these results are considerably influenced by the heating rate. The aging effect, see Stephan (1992), is a complex problem which is not yet very well understood.

Table 2. Nucleation data

Surface	Orientation	Average heat flux	Temperature	$\Delta T = T_w - T_{sat}$ (K)	T_{bulk} (°C)
S: smooth	V: vertical	q (kW/m ²)	Location		
G: grooved	H: horizontal				
S	V	14.7	Average	16.0	20.0
S	V	17.8	Average	15.1	22.0
S*	V	12.2-20.77	Average	7.6	26.0-33.2
G	V	11.0	Average	8.7	22.9
G	V	4.3	Average	7.8	44.1
S	H	3.6	Bottom	11.4	46.0
			Top	12.4	
G	H	3.8	Bottom	8.7	40.0
			Top	9.7	

(*) In this line the average value of ΔT is provided, corresponding to eight different tests. Four tests were performed on February 02 and four on March 02 2000. ΔT is comprised within the interval ranging from 4.9 to 10.2 K.

3.2 Nucleate boiling

Figures 4a and 4b show experimental pool boiling curves for the smooth and grooved tubes, respectively, at different values of bulk liquid temperature and for heat flux up to 45 kW/m². As it may be observed in Figure 4a, the difference between wall temperatures for tests at 47 °C and 23 °C, for a same heat flux, is approximately 5°C in the nucleate pool boiling region, which corresponds to the heat flux region higher than 15 kW/m² when T_{bulk} equals 23.0 °C and higher than 5 kW/m² when T_{bulk} equals 44.0 and 47.0 °C. This difference in wall temperatures is also

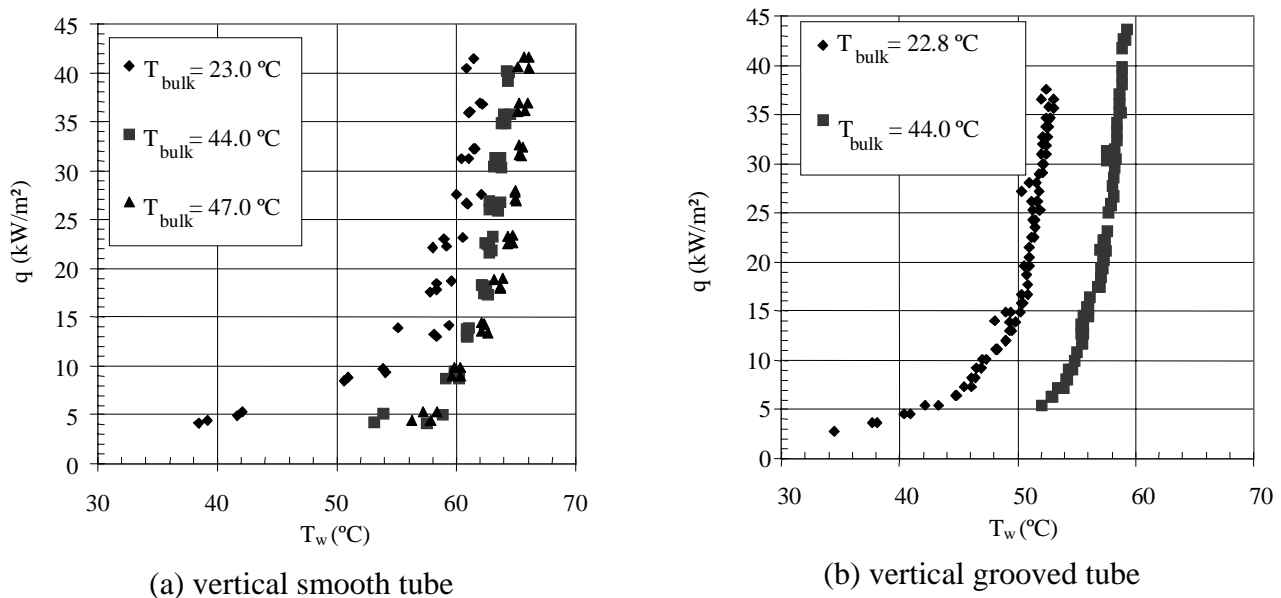


Figure 4 – Effect of the bulk temperature

observed for tests at 44 and 28 °C, for the grooved tube. This means that, even for an increase in fluid temperature higher than 20°C, wall temperature increase is not higher than 5 °C. These results are in line with Carey’s (1992) observations about the no effect of bulk liquid temperature on the nucleate pool boiling regime for high heat flux region. In fact, the heat flux in the present work may be considered moderate when compared to the critical heat flux value of about 200 kW/m² which would be expected for the geometry, working fluid and test conditions of this study.

Figures 5a-b show the results of surface effect on pool boiling curves for subcoolings equal to 24.6 and 24.8 °C, in Fig. 5a, and 3.5 and 3.6 °C, in Fig. 5b. For high subcooling, Fig. 5a, and in the region under natural convection, for heat flux smaller than 5 kW/m², wall temperature is independent of the surface tube, whereas, under the nucleate boiling, for heat flux higher than 15 kW/m², wall temperatures differ in nearly 8 °C, with the grooved tube exhibiting the lowest temperatures. These results confirm the enhancement of nucleate boiling heat transfer when the surface is grooved.

Figures 6a-b show the heat flux as a function of wall temperatures, at the bottom, middle and top of the smooth tube, for $T_{bulk} = 47.5$ °C, and the grooved tube, for $T_{bulk} = 45.5$ °C, in the horizontal orientation. Both figures show the existence of a temperature gradient, in the azimuthal direction of the aluminum tube, with a lower temperature at the top region. This result was considered by Passos & Reinaldo (2000), in the case of the smooth tube, as an effect of the existence of different mechanisms of boiling on the tube wall. At the top region, there was an elongated bubble, whereas on the side and bottom isolated bubbles were found. The existence of an elongated bubble promoted the vaporization of a liquid film between the wall and the bubble with the improvement of the heat transfer mechanism in this region. For the grooved tube, temperature differences between the bottom and the top are nearly 8 °C for heat fluxes higher than 25 kW/m². The same mechanisms described above are also present in the grooved tube and, in addition, there is a cooling effect of the transport of the liquid through the grooves. Moreover, as in the case of vertical orientation, the boiling is enhanced by the grooved surface.

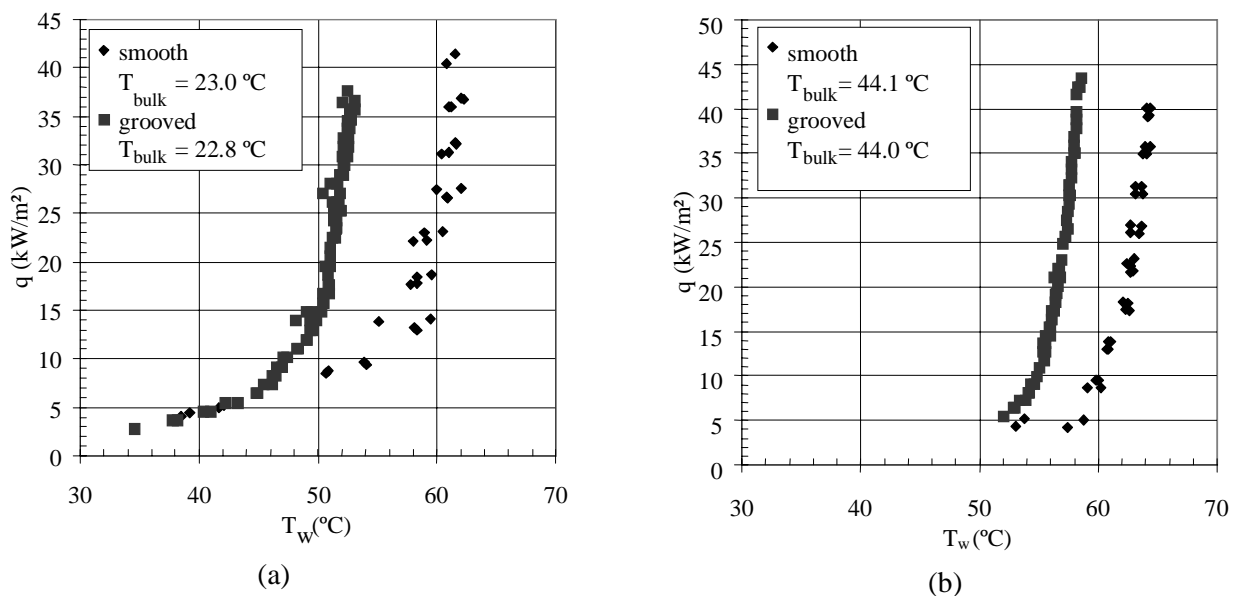
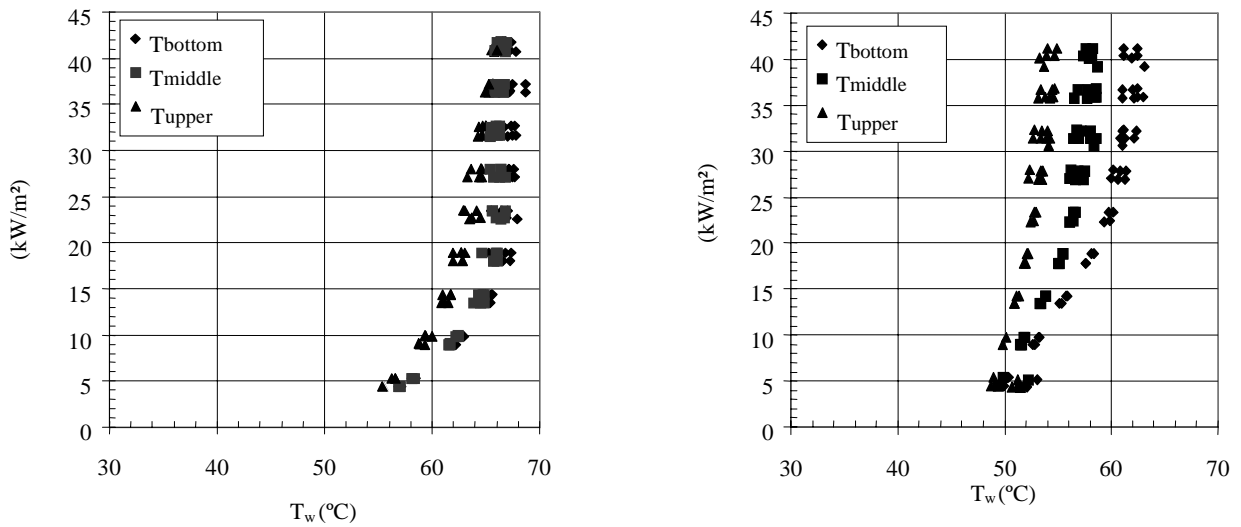


Figure 5 – Effect of the tube surface



(a) Horizontal smooth tube, $T_{\text{bulk}} = 47.5^\circ\text{C}$

(b) Horizontal grooved tube, $T_{\text{bulk}} = 45.5^\circ\text{C}$

Figure 6. Pool boiling curves for horizontal tubes

3.3 Correlation analysis

Figure 7 shows the comparison between the experimental boiling heat transfer coefficient for the vertical smooth tube at $T_{\text{bulk}} = 47^\circ\text{C}$ and the h values computed by the correlations of Stephan and Abdelsalam, Cooper, Rohsenow (using 2 values of the exponent s , 1 and 1.7) and Forster and Zuber. The first two correlations consider the effect of wall roughness, which is equal to $2.2\ \mu\text{m}$. It is observed that the correlations of Stephan and Abdelsalam, Cooper and Rohsenow ($s=1$) agree between them and furnish h values greater than those found experimentally. h values obtained by Forster and Zuber correlations tend to agree with the experimental values of h in the region of high heat flux. Rohsenow correlation ($s=1.7$) estimates h values smaller than the experimental h values.

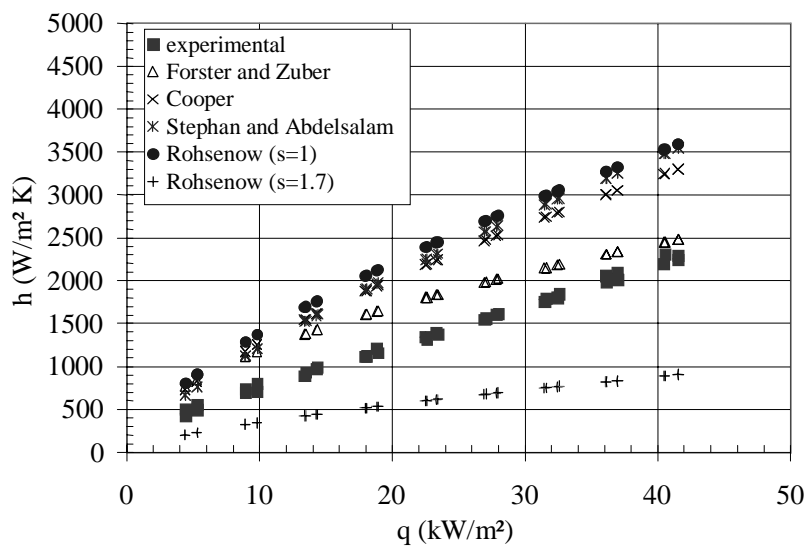


Figure 7 – Heat transfer coefficients (vertical smooth tube, $T_{\text{bulk}} = 47^\circ\text{C}$)

4. CONCLUSIONS

This work summarizes results obtained in a Master of Science program developed at the Department of Mechanical Engineering of the Federal University of Santa Catarina, (Reinaldo, 1999).

Nucleation results for horizontal orientation show higher wall temperatures at the upper part of the tube compared with the bottom, during natural convection, and these temperatures revert after the onset of boiling. Superheating values for the smooth tube were found to be either smaller, equal or higher than results for the grooved tube.

For the nucleate regime, under moderate heat flux ($q < 45 \text{ kW/m}^2$), pool boiling heat transfer is not so dependent on liquid bulk temperature. The nucleate regime was enhanced by the grooved surface.

The existence of isolated and elongated bubbles on the wall, inside the horizontal tubes, promotes a more efficient heat transfer at the top region, where the temperature is lower than the temperatures at the middle and bottom of the tube.

The experimental heat transfer coefficient, for the smooth tube, with R113 bulk temperature, is lower than the values computed by the correlations of Stephan and Abdelsalam, Cooper, Rohsenow (with $s=1$) and Forster and Zuber. For a heat flux of approximately 40 kW/m^2 , experimental results tend to agree with the values computed by the Forster and Zuber correlation.

Acknowledgments

The authors wish to thank CNPq, CAPES and the Brazilian Space Agency (AEB) for the financial support received.

REFERENCES

- ASME, 1986, Measurement Uncertainty, ANSI/ASME Powe Test Code 19-1-1985/ASME, New York.
- Carey, V. P., 1992, Liquid-Vapor Phase-Change Phenomena: An Introduction to the Thermophysics of Vaporization and Condensation in Heat Transfer Equipment, Taylor and Francis.
- Cooper, M. G. , 1984, Saturation Nucleate Pool Boiling – A Simple Correlation, International Chemical Engineering Symposium Series, vol. 86, pp. 785-792.
- Forster, H. K., Zuber, N. , 1955, Dynamics of Vapor Bubbles and Boiling Heat Transfer, A.I.Ch.E Journal, vol. 1, n. 1, pp. 531-535.
- Hewitt, G. F., 1998, Boiling, Editors, W. M. Rohsenow et al., Chapter 15, McGraw Hill.
- Holman, J. P., 1989, Experimental Methods for Engineers, McGraw-Hill, New York.
- Kline, S. J., 1985, The Purposes of Uncertainty Analysis, ASME Journal of Fluid Engineering, vol. 107, pp. 153-160.
- Marto, P. J. & Lepere, J., 1982, Pool Boiling Heat Transfer from Enhanced Surfaces to Dielectric Fluids, J. Heat Transfer:Transactions of the ASME, vol. 104, 292-299.
- Passos, J. C. & Reinaldo, R. F., 2000, Analysis of Pool Boiling within Smooth and Grooved Tubes, To be published in ETF - Int. J. Experimental Thermal and Fluid Science, 10 pages.
- Reinaldo, R. F., 1999, Experimental Study of the Nucleate Boiling on Smooth and Grooved Cylindrical Surfaces, in Portuguese, M. Sc. Dissertation, Graduate Program on Mechanical Engineering, Federal University of Santa Catarina, Brazil.
- Stephan, K., 1992, Heat Transfer in Condensation and Boiling, Springer-Verlag.
- Stephan, K. & Abdelsalam, M., 1980, Heat-Transfer Correlations for Natural Convection Boiling, Int. J. Heat Mass Transfer, vol. 23, pp. 73-87.
- Thome, J. R., 1990, Enhanced Boiling Heat Transfer, Hemisphere Publishing Corp., Washington, D.C.